5-11-2022

Predicting RF Signal Degradation Through the Hypersonic Plasma Sheath Using dsmcFoam and PIC Method

Andrew DeRubertis

Ramesh K. Agarwal
Washington University in St. Louis

Predicting RF Signal Degradation Through the Hypersonic Plasma Sheath Using dsmcFoam and PIC Method

Andrew J. DeRubertis* and Ramesh K. Agarwal†
Washington University in St. Louis, St. Louis, MO, 63130

The transmission and degradation of RF signals through the plasma sheath surrounding hypersonic vehicles is investigated using a DSMC flow solver method. The OpenFoam library dsmcFoam is used to simulate flow around hypersonic bodies and obtain flow field properties to aid in calculations of signal degradation. The study of RF signal degradation and the viability of communications for hypersonic vehicles is of supreme importance for the future of aerospace as hypersonic travel and warfare is becoming technologically possible. Integrating over the output electron number density profile yields values for attenuation that drop below 100 decibels in the transmission window of 10 to 30 GHz. In this window, phase shift values remain between 2 and 10 radians. Outside of this transmission window, attenuation and phase shift are high and indicate poor chance of viable communications. If signal degradation models can be verified and improved with wind tunnel and flight data, these results suggest that vital radar and satellite communications are possible through the plasma sheath and can be decoded using accurately predicted degradation values.

I. Nomenclature

w_p	=	plasma frequency $[\frac{rad}{s}]$
w	=	transmitted signal frequency [Hz]
v	=	velocity $[\frac{m}{s}]$
c	=	speed of light $[\frac{m}{s}]$
T	=	attenuation [dB]
α	=	attenuation per unit length $[\frac{db}{m}]$
β	=	phase shift per unit length $[\frac{rad}{m}]$
ν_e	=	particle collision frequency
k	=	Boltzmann constant
T_e	=	electron Temperature [K]
n_d	=	species number density $[\frac{}{cm^3}]$
n_e	=	electron number density $[\frac{}{cm^3}]$
n_0	=	ion number density $[\frac{}{cm^3}]$
Kn	=	Knudsen Number
λ	=	mean free path [m]
L_{char}	=	characteristic length [m]

II. Introduction

In the past, hypersonic research was mostly focused in astronautics and understanding reentry flow. In the last decade, hypersonics has grown and sparked broad interest from the fields of aerospace and aeronautics. Thanks to improvements in simulation software [and computing power], aircraft material development, and high speed propulsion, hypersonic weapons, reconnaissance drones, and demonstration vehicles have come into intense focus across the world. Hypersonic research projects such as NASA's X-43 series, Boeing and AFRL's X-51A, and Lockheed Martin and DARPA's HTV-2 are examples of the acceleration of hypersonics and the need for test flight data. Current advancement

*Aerospace Engineering M.S. Student, Washington University in St. Louis, 1 Brookings Drive, St. Louis, MO 63130.
†William Palm Professor of Engineering, Washington University in St. Louis, 1 Brookings Drive, St. Louis, MO 63130., and AIAA Member Grade (if any) for second author.

in hypersonic capabilities require facing the complex challenges of heat ablation, extreme surface temperatures and heat fluxes, sustaining ramjet and scramjet propulsion, and plasma formation and communication loss.

One of the many challenges in the electromagnetic interference [EOI] arena of hypersonics is the plasma sheath that forms around the vehicle and the difficulty of flight data and communications to pierce this shield. This problem has been present since space flight was first possible. Reentry vehicles experience radio blackout with ground communications because of the plasma sheath. Engineers have considered many solution paths to the blackout problem including sensor location and magnetic sensor windows [1]. Changing sensor locations has aerodynamic constraints, and magnetic sensor windows run into material constraints [1]. One solution path that has only been investigated on the surface, is improving calculations of signal degradation in the plasma sheath itself. Theoretical equations exist in research that integrate along the line of sight through a dense electron field to obtain attenuation and phase shift values [2]. This report outlines research undertaken to use DSMC flow simulation and PIC plasma modeling in conjunction with these equations and an altered integration method to calculate attenuation and phase shift values of RF signals transmitted from a hypersonic vehicle.

Any communication below the critical plasma frequency is completely destroyed [3]. RF signals above the critical plasma frequency are attenuated and undergo a phase shift, but theoretically they can pierce through the sheath and transmit to the receiver, albeit arriving as degraded signals. It is possible that these degraded signals could be reconstructed and decoded. Currently, no model is able to accurately calculate the attenuation and phase shift of transmitted RF signals through dense, hypersonic plasmas. The quest to successfully calculate these extremely complex values begins with obtaining species density profiles in the plasma sheath, specifically of the electron number density. Due to the scarcity of hypersonic test flight data and the difficulty in replicating extremely high temperature conditions in wind tunnels, obtaining these profiles via computer simulation is integral to understanding signal transmission from hypersonic aircraft.

III. Numerical Setup

Direct Simulation Monte Carlo, widely known as DSMC, is a numerical fluid solver that solves the Boltzmann equations non-deterministically. Rather, DSMC is a stochastic method that solves Boltzmann's equations by sampling from a Maxwellian distribution of simulation particles to find and execute possible collisions in mesh cells in the domain. This method was fathered by Graeme Bird in the 1960's, and is one of the principal solvers used for rarefied gas flows [4]. The reason this method and others similar to it are so important, is that at high Knudsen numbers, the Navier Stokes equations break down, because they govern continuum fluid mechanics. High Knudsen numbers correspond to rarefied flows, where the mean free path is much larger than the characteristic length. Mathematically,

$$Kn = \frac{\lambda}{L_{char}} \tag{1}$$

where L_{char} is the characteristic length. In plasma flow, the overall Knudsen number uses a characteristic length equal to the thickness of the plasna. Local Knudsen number uses the diameter of a particle of interest to be the characteristic length [5]. These types of flows are non-continuum, and therefore rely on the Boltzmann molecular model, rather than the Navier-Stokes continuum model. dsmcFoam is an open-source CFD library built in the OpenFoam framework, and it was the primary CFD software used for this work. dsmcFoam has been validated and compared to other well-known and accepted DSMC solvers in academia and industry [6].

The other numerical approach used in the particle in cell, or PIC, method. This method is similar to DSMC in that is uses simulation particles to represent real particles, but now includes ions and electrons [7]. The method includes electromagnetic forces on charged partices. Because of these capabilities, the PIC method is well-suited for plasma simulation and modeling. From this method, an accurate electron number density around the body can be obtained.

The Boltzmann Equations are conservative meaning that mass, momentum, energy, and species are conserved [8]. The Boltzmann equation calculates a particle distribution based on post-collision velocities, diffusion rates, and external forces such as an electric or magnetic field [8]. One important cability of using DSMC *and* PIC is the ability to use the Boltzmann relationship to obtain an electron model, and then use the electromagnetic field to account for external forces on charged ions in the solver. Boltzmann's relationship comes from combining Poisson's Equation and the equation for electron momentum. Poisson's equation relates the electric potential field to the charge density and therefore ion density [7]. Combining this with the integrated electron momentum equation to relate potential, ϕ, and the electron field yields the Boltzmann relationship which follows

$$e(\phi - \phi_0) = k * T_e * \ln \frac{n}{n_0} \tag{2}$$

This can be rearranged to express the electron number density as

$$n_e = n_0 * \exp \frac{\phi - \phi_0}{kT_e} \tag{3}$$

Without using the combination of methods, DSMC makes the assumption that the electron number density is approximately equal to the ion number density in the flow. This does not account for electromagnetic forces.

In the post-processing step, the line of sight integration through the plasma sheath is performed in MATLAB, and also translated to Python. With the non-uniform mesh that will be discussed further in the next section, the difficulty in the post-processing step is to find the data points of cells that are closest to the line of sight. Once these points that lay along the line of sight are obtained by a function minimizing the Euclidean distance, the electron number density at these points and the distance between these points is used in a quasi-trapezoidal integration step. In MATLAB, the code allows for the user to choose points in the domain that define the line of sight. In Python, the user can input latitude and longitude coordinates, with the altitude being fixed at 95,000 ft. This lat/lon extension is also being worked on for the MATLAB code.

A. Post-processing Step

Fig. 1 shows a closer look at the post-processing step in MATLAB.

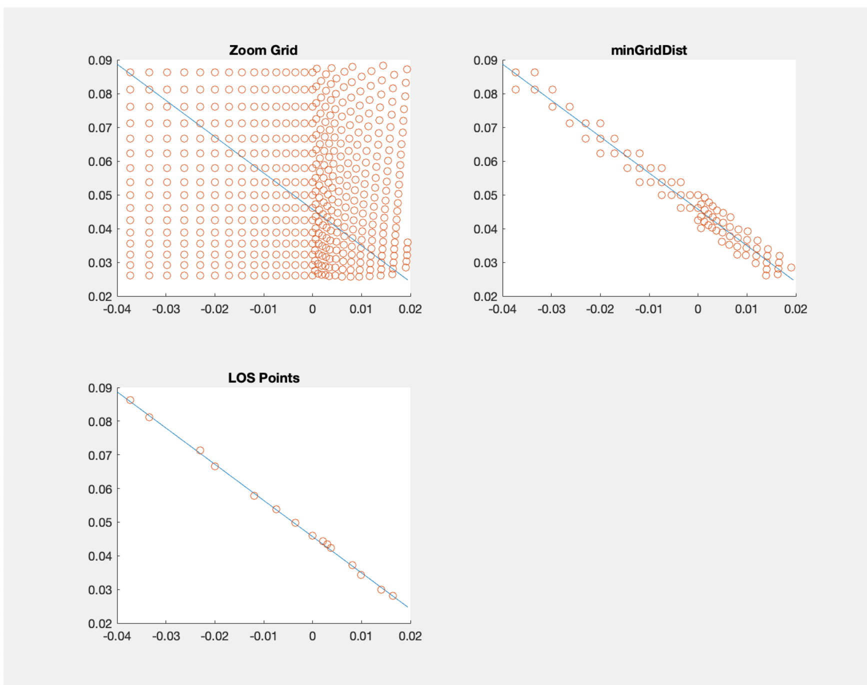

Fig. 1 Selection of closest data-points to line of sight for quasi-trapezoidal integration method

The 'Zoom Grid' plot shows the data points that are read into the file along the line of sight. The 'minGridDist' plot shows the points that are within some user-defined threshold distance from the line of sight. The 'LOS Points' plot shows the 15 closest data-points to the line of sight by Euclidean distance. Choosing 15 points was arbitrary, but seemed to capture the best results any fluctuations in less dense regions of the mesh.

The Yang Model follows [2]

$$A = \int_a^b \alpha ds \tag{4}$$

$$B = \int_a^b \beta ds \tag{5}$$

A is attenuation. B is phase shift. s is length along the line of sight. α and β follow

$$\alpha = \frac{w}{\sqrt{2} * c} * \sqrt{\frac{w_p^2}{w^2 + \nu_e^2} - 1 + \sqrt{(1 - \frac{w_p^2}{w^2 + \nu_e^2})^2) + (\frac{\nu_e}{w} * \frac{w_p^2}{w^2 + \nu_e^2})^2}} \tag{6}$$

$$\beta = \frac{w}{\sqrt{2} * c} * \sqrt{1 - \frac{w_p^2}{w^2 + \nu_e^2} + \sqrt{(1 - \frac{w_p^2}{w^2 + \nu_e^2})^2) + (\frac{\nu_e}{w} * \frac{w_p^2}{w^2 + \nu_e^2})^2}} \tag{7}$$

The Lin Model is similar, derived from the same propagation constant, but differs slightly [9]. It follows

$$A = \int_a^b \alpha ds \tag{8}$$

$$B = \int_a^b \beta ds \tag{9}$$

A is attenuation. B is phase shift. s is length along the line of sight. α and β follow

$$a = \sqrt{1 - \frac{\frac{w_p}{w}^2}{(1 + (\nu/w)^2})^2 + (\frac{w_p}{w})^2 * (\frac{\nu}{w})/(1 + (\frac{\nu}{w})^2)^2} - (1 - (\frac{w_p}{w})^2/(1 + (\frac{\nu}{w})^2) \tag{10}$$

$$\alpha = \sqrt{\frac{a}{2}} * \frac{w}{c} \tag{11}$$

$$b = \sqrt{1 - \frac{\frac{w_p}{w}^2}{(1 + (\nu/w)^2})^2 + (\frac{w_p}{w})^2 * (\frac{\nu}{w})/(1 + (\frac{\nu}{w})^2)^2 - (1 - (\frac{w_p}{w})^2/(1 + (\frac{\nu}{w})^2)} \tag{12}$$

$$\beta = \sqrt{\frac{b}{2}} * \frac{w}{c} \tag{13}$$

IV. Physical Model and Mesh

The hypersonic bodies simulated were an inclined surface and an elliptic nose cone body with a length of .5 m and height of .2 m. The simulation was two-dimensional. The mesh was non-uniform, growing more refined near the leading edge, and coarser in the far-field. The mesh contained 200,000 cells.

Because the DSMC method uses the stochastic process of sampling a distribution of simulated particles in each cell, the mesh does not need to be as refined as the mesh for typical continuum solver methods like Navier-Stokes. Rather, there is a condition that must be met to ensure the probabilistic model is valid for real collisions. Each cell's width and height, dx and dy, must be smaller than one third of the mean free path [10]. The relation follows,

$$dx, dy < \frac{\lambda}{3} \tag{14}$$

The mean free path, λ, is the average distance a particle will travel before a collision. It changes with altitude, because atmospheric density changes. At 95,000 ft, the altitude of the simulation and with which the flow boundary conditions are defined, the mean free path is about 1.5 mm [5]. Therefore, the largest mesh cells do not have a width or height grater than 0.5 mm. This discretization requirement ensures that within a cell, a collision will definitely occur. If spatial discretization were such that collisions will not occur in a cell because of a larger mean free path, then the method would be sampling for collisions that are not likely to occur over the given distance. Choosing a maximum width or height of one third of the mean free path solves this potential problem.

V. Results and Discussion

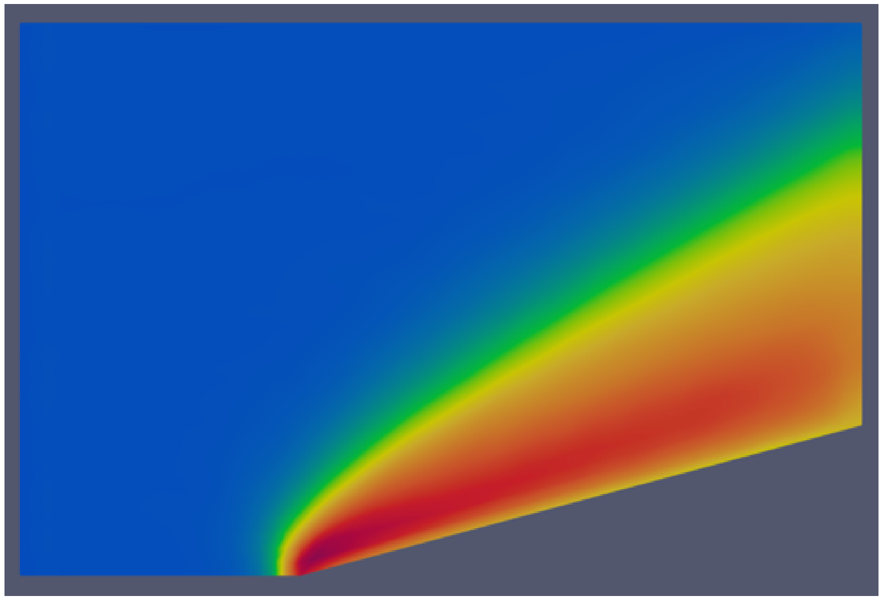

Fig. 2 Number Density around surface of an inclined wedge body in hypersonic flow

Fig. 2 shows the electron number density profile around an inclined surface body. The maximum electron number density seen in the plasma was 5.4e+20 $/m^3$. An arbitrary line of sight was chosen close to where the plasma is thickest to measure worst-case signal degradation. The RF signal was considered to be transmitted with a frequency of 10 GHz from one tenth of the length from the leading edge at a 45 degree angle from the negative x axis. In the Yang model, this signal yielded an attenuation value of 78.6 decibels and a phase shift of 8.2 radians. In the Lin model, this signal yielded an attenuation of 47.1 decibels and a phase shift of 2.8 radians.

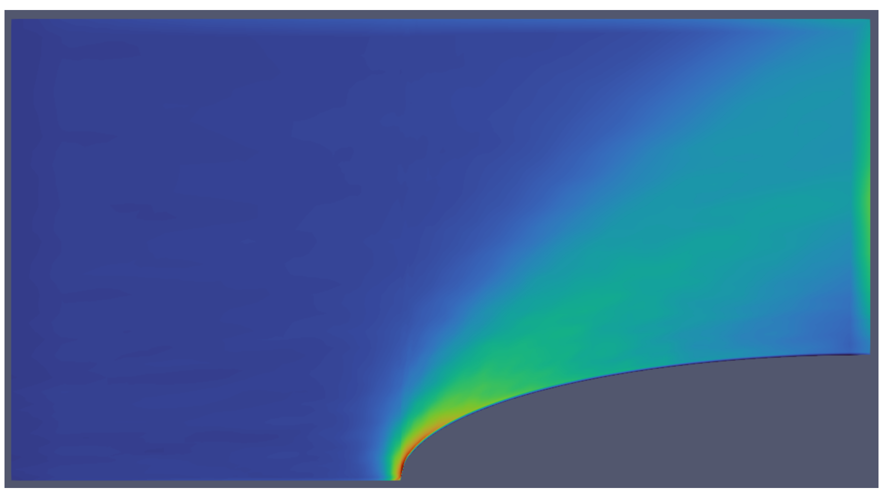

Fig. 3 Number Density around surface of elliptic body in hypersonic flow

Fig. 3 shows the electron number density profile around the elliptic body. The maximum electron number density seen in the plasma was 1.1e+21 $/m^3$. Again, an arbitrary line of sight was chosen close to where the plasma is thickest to measure worst-case signal degradation. The RF signal was considered to be transmitted with a frequency of 10 GHz from the surface at the point where y equals one tenth of the height of the body, $y = .02$ m, and at a 30 degree angle from the negative x axis. In the Yang model, this signal yielded an attenuation value of 82.4 decibels and a phase shift of 9.1 radians. In the Lin model, this signal yielded an attenuation of 66.8 decibels and a phase shift of 3.4 radians.

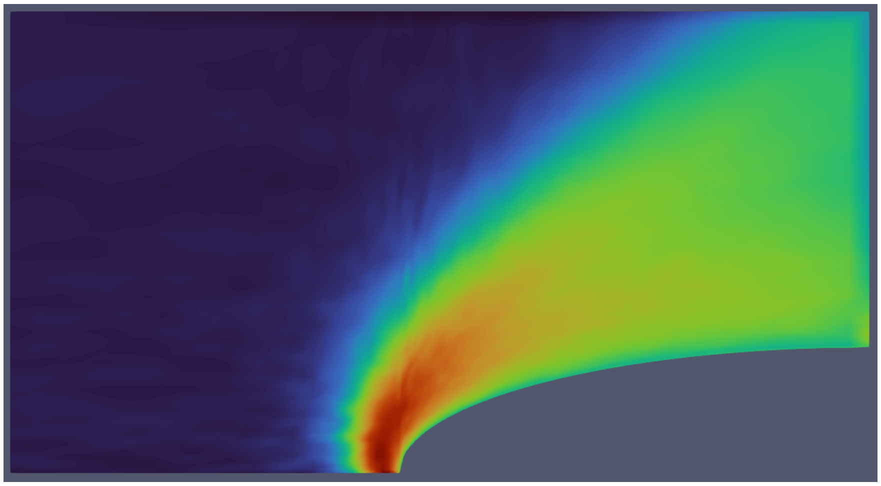

Fig. 4 Temperature around surface of elliptic body in hypersonic flow

Fig. 4 shows the temperature profile around the elliptic body in hypersonic flow at 95,000 ft. The maximum temperature near the leading edge was 1500 K.

Fig. 5 Pressure around surface of elliptic body in hypersonic flow

Fig. 5 shows the pressure around the elliptic body in hypersonic flow. The pressure profile shows shock separation near the top of the body towards the outlet of the computational domain. This separation can also be seen in the electron number density profile in 3. The shock separation seen is expected in hypersonic flow.

VI. Conclusion

This research serves as a successful first step towards integrating a DSMC flow solver with a PIC solver and post-processing with RF degradation models in mind to predict signal degradation through the hypersonic plasma sheath. The decreased attenuation and phase shift in the SHF RF band suggest that vital radar and satellite communications may be possible through the plasma during hypersonic flight. The effects of sensor degradation and heat ablation on signal transmission are ignored, but can be introduced and overlapped in future work. With improved parallel processing tools, the next iteration of this research may include utilizing parallel processing to solve electrons as kinetic particles, instead of superimposing the Poisson derived electron density based on the electric potential that comes from DSMC. Other well-known CFD softwares like NASA's DAC software also implement the DSMC method for hypersonic flow, and these simulation models can be compared in future iterations of work to establish a firmer idea of model fidelity, even without test flight data. NASA's DAC software also introduces adaptive meshing to the DSMC solver infrastructure, which is an important next step in all turbulent flows, enhancing mesh refinement around large pressure gradients. Finally, introducing wind tunnel, but more importantly test flight data to compare with these models would make this research industry-ready and highly important for the future of hypersonic communications. Because this is so for maintaining communications with any hypersonic vehicle or projectile, improvement of this model and expansion of this research is integral to the future of aerospace. The industry as a whole can not continue to rely on Navier Stokes flow solver to handle the non-continuum rarefied flows present in the hypersonic regime.

Acknowledgments

I would like to thank Dr. Agarwal for his guidance and tutelage through my research - it would not be possible without his expertise. I would also like to thank the entire MEMS Department at the McKelvey School of Engineering at Washington University in St. Louis for allowing me to pursue this independent study course. I am very grateful to be pursuing my degree at a top engineering school in the country that allows me to do so through research that I am highly passionate about. And of course, I would not be where I am today without my family and close friends and their undying support for me.

References

[1] Gillman E., B. I., Foster J., "Review of Leading Approaches for Mitigating Hypersonic Vehicle Communications Blackout and a Method of Ceramic Particulate Injection Via Cathode Spot Arcs for Blackout Mitigation," , 2010. URL https://ntrs.nasa.gov/api/citations/20100008938/downloads/20100008938.pdf.

[2] Yang, M. e. a., "Propagation of Phase Modulation Signals in Time Varying Plasma," , 2016. URL https://aip.scitation.org/doi/10.1063/1.4950694.

[3] Mackey L., B. I., "Analysis of Hypersonic Flow Effects on Sensor Performance," , 2016. URL https://deepblue.lib.umich.edu/bitstream/handle/2027.42/140623/6.2016-4103.pdf?sequence=1.

[4] Bird, G., "The DSMC Method," , 2013.

[5] Schouler, P. Y., M., "Survey of flight and numerical data of hypersonic rarefied flows encountered in Earth orbit and atmospheric reentry," , 2020. URL https://www.researchgate.net/publication/344332781_Survey_of_flight_and_numerical_data_of_hypersonic_rarefied_flows_encountered_in_Earth_orbit_and_atmospheric_reentry.

[6] White, e. a., C., "dsmcFoam+ An openFOAM based direct simulation Monte Carlo Solver," , 2017. URL https://www.sciencedirect.com/science/article/pii/S0010465517303375.

[7] Brieda, L., "Particle In Cell," , 2012. URL https://www.particleincell.com/2010/es-pic-method/.

[8] Hagellar, P. L., G.J., "Solving the Boltzmann equation to obtain electron transport coefficients and rate coefficients for fluid models," , 2005. URL https://iopscience.iop.org/article/10.1088/0963-0252/14/4/011/meta.

[9] Lin TC, S. K., "Influence of reentry turbulent plasma fluctuation on EM wave propagation," , 2006. URL https://www.sciencedirect.com/science/article/abs/pii/S0045793006000077.

[10] Pikus, A., "DSMC/SPARTA Lecture 1," , 2019. URL https://www.youtube.com/watch?v=cSFr8MTr30Y&t=1687s.